Journal of Advanced Laboratory Research in Biology
E-ISSN: 0976-7614
Volume 7, Issue 2, 2016
PP 52-65
https://e-journal.sospublication.co.in

Research Article

Ultra-differentiation of Sperm Head in Lesser Egyptian Jerboa, *Jaculus jaculus* (Family: Dipodidae)

Osama Mohamed M. Sarhan*

Department of Zoology, Faculty of Science, Fayoum University, Egypt.
Department of Biology, Faculty of Applied Science, Umm Al-Qura University, KSA.

Abstract: In the present study, events of sperm head differentiation in Lesser Egyptian Jerboa, *Jaculus jaculus* were studied for the first time. Adult males of *J. jaculus* were collected during their period of sexual activity from sandy regions of Marsa-Matrouh at northwest of Egypt. Tissues of their testes were prepared for ultrathin sections, which examined under a Joel "JEM-1200EXII" operating at 60-70kv. Early and late spermatids were photographed to describe the successive stages of sperm head differentiation.

Early spermatids have rounded or oval nuclei with fine chromatin granules and their cytoplasm showed numerous mitochondria, one or more chromatoid bodies and segments of rough endoplasmic reticulum. The first stage of spermatid development usually starts when the Golgi body produces secretory vesicles. These vesicles usually differentiate into an oval dense acrosomal granule, the rest forming a thin layer of acrosomal cap which extends to cover the anterior half of the nucleus and stop on at the nuclear shelf in the equatorial nuclear region. This cap is separated from the nuclear envelope by a narrowed subacrosomal space. Novel and complex structures are observed in the developing acrosome, which is, the crown, anterior, and posterior acrosomal segments, anterior and posterior acrosomal caps, as well as a long dorsal and a short ventral acrosomal caps; posterior subacrosomal spaces and subacrosomal cone at the tip of the elongated nucleus.

Cytoskeletal elements are responsible for re-shaping of the nucleus. A light comprehensive strength of cytoskeletal elements usually induces nuclear prolongation and formation of implantation fossa that appears in the ventrodorsal region at the posterior side of the nucleus. Manchette microtubules, solitary microtubules, and microfilaments may generate gentle compressive strength to accelerate nuclear prolongation.

Manchette microtubules, which disposed of parallel to one another and to the long axis of the nucleus, could exert the force, required to produce the spermatid nucleus elongation forward and perhaps backward and to protect DNA during nuclear condensation. A translucent space appears to surround the posterior half of the nucleus in order to mitigate the pressure on the nucleus and regulate the elongation with the protection of genetic material during nuclear condensation. Worth mentioning, that the translucent perinuclear space is a unique structure was not described or discussed before.

Keywords: Ultra-structure, Sperm head, Lesser Egyptian Jerboa, *Jaculus jaculus*, Rodents.

1. Introduction

In the mammalian seminiferous tubules, two stages in which spermatogenic cells produced male gametes by way of mitosis and meiosis. First, known as spermatocytogenesis, spermatogonia developed into spermatids; the second is called spermiogenesis, spermatids reformed into spermatozoa [1].

After second meiotic division, Spermatids derives from the division of secondary spermatocytes and undergoes a series of morphological and cytological changes leads to formation of fully developed spermatozoa. Under the subcellular level, stages of the sperm head and/or sperm tail differentiation were taken into consideration by the scientists [2-7]. In mammalian spermiogenesis, the nucleus of spermatid becomes elongated; its chromatin condensed; the anterior nuclear protrusion is capped by acrosome [6-7]; the centrioles migrate to the prospective posterior end of the nucleus then situated into a depression, nuclear implantation fossa, where the connecting piece, mitochondrial and fibrous sheath are formed followed by extension of an axial filament surrounded by a special fibrous sheath [8].

*Corresponding author:
E-mail: sarhanomm5975@gmail.com.

Publications interests of spermiogenesis are focused on several themes include differentiation of normal and abnormal sperm head [2] and/or sperm-tail [12,15] as well as other detailed investigations directed to study the role of some organelles such as Golgi apparatus [3-7], microtubules [8-12] and chromatoid bodies [13] involved in the formation of acrosome [14], manchette formation of spermatid cytoskeleton according to sperm needs [10-13], and configure the fibrous sheath [15-20] along the axial filament [21] in the human [22,23] and mammalian spermatozoa [24-31].

In order Rodentia [32-35], few investigations are dealt with the ultrastructure of sperm head or sperm tail differentiation, especially in Egyptian fauna [36-38]. Moreover, the mechanisms of the interesting formative events in sperm head of Egyptian mammals are still eluding the present researcher. This work aimed to investigate specific characterization of sperm head differentiation in the Lesser Egyptian Jerboa, *Jaculus jaculus* as one of the threatened species [39].

2. Material and Methods

2.1. Animals

Adult males of *J. jaculus* were collected during their period of sexual activity from sandy regions of Marsa-Matrouh at northwest of Egypt.

2.2. Tissue preparation

After light ether anesthesia, testes were immediately extracted, washed in cacodylate buffer solution adjusted at pH 7.2, cut into two halves and fixed in 2.5% glutaraldehyde in the refrigerator. 2 hours later, thin slices were taken and cut into smaller specimens (about 0.5-1.0mm thick), rewashed in fresh cold buffer to remove depressed tissues and transferred again into fresh cold 2.5% glutaraldehyde for 4-6 hours. The fixative removed, and specimens washed 3 times in buffer and post-fixed 3 hours in 1% osmium tetroxide buffer, then washed in buffer followed by dehydration, clearing using propylene oxide and embedding in Epon-Araldite mixture.

Semithin sections about 1µm thick were taken, stained using toluidine blue, examined under light microscope to select best locations of spermiogenesis activities, especially sites of sperm head differentiation. Ultrathin sections were stained using aqueous uranyl acetate (1.5%) and lead citrate then examined under a Joel "JEM-1200EXII" operating at 60-70kv. Early and late spermatids were observed and magnified and photographed to describe successive stages of sperm head differentiation.

3. Results

In the seminiferous tubules, the epithelium consists of sustentacular cells known as Sertoli cells (Ser), which are tall, columnar type cells that line the tubules and spermatogenic cells, which differentiate through meiosis to spermatids and subsequently undergoes morphological stages to form sperm cells (Fig. 1). Early spermatids have rounded or oval nuclei with fine chromatin granules and their cytoplasm showed numerous mitochondria (M), one or more chromatoid bodies (CB) and segments of rough endoplasmic reticulum (RER) (Fig. 2). The first stage of spermatid development usually starts when Golgi body (G) produces secretory vesicles (SV) (Figs. 3, 4). These vesicles usually differentiate into an oval dense acrosomal granule (AG), the rest forming a thin layer of acrosomal cap (AC) which extends to cover the anterior half of the nuclear membrane and separates from it by a narrowed subacrosomal space (SAS). This cap surrounds the anterior half of nuclear envelope and stops on at the nuclear shelf (NS) (Fig. 5). The next stages show the nuclear re-shaping, chromatin condensation, reformation of cytoskeleton, completion of acrosome (Figs. 6-20) and other regions of the developing sperm.

3.1 Role of manchette in the shaping of the sperm nucleus

Mainly, the cytoskeleton in active spermatid is formed of microtubules and microfilaments (Figs. 3, 5, 7). They pass in circular pathways, thus, they are distributed under the cell membrane, in the cytoplasm and around the nuclear envelope (Figs. 3-5). Some elements of cytoskeleton re-orient the posterior end of nuclear envelope to form a posterior concavity, implantation fossa, to lodge the proximal centriole (Fig. 5). Figure 6 proves that this concavity appears in the posterior ventromedial side of the nucleus. Another large unit of microtubules (MtU) move to surround the equatorial of the nucleus at the nuclear shelf (NS) where the acrosomal cap stops on (Fig. 7). At this point, front half of circular microtubules that surround the nucleus are reduced pushing the cell organelles backwardly, at the same time; some of the posterior half microtubules attach themselves to the MtU, re-oriented parallel to one another and to the long axis of the nuclear envelope then end at the rear when docking with the basal plate (BP). In addition, some solitary smaller microfilaments are arranged in a transverse direction to surround the posterior perinuclear space (PP) that first appears along then surround the posterior ventral side of the nucleus (Figs. 8-13). Both MMs, solitary Mts and microfilaments (Mfs) may be generated gentle compressive strength for the nucleus elongation forward and perhaps backward and to protect DNA during nuclear condensation. A translucent space appears to surround the posterior half of the nucleus in order to mitigate the pressure on the nucleus and regulate the elongation with the protection of genetic material during nuclear condensation (Fig. 8). At the present stage, nuclear condensation starts in

parallel with nuclear elongation. Next stage showed that MMs extend to the posterior side of the nucleus and unite with the basal plate (BP) at the posterior nuclear shelf (PNS) that shown in Figs. 8-13. Also, numerous Mfs appear on a single or double row surrounding the posterior half of the nucleus as they run in a circular path (Fig. 9).

In late spermatid, as shown in Figs. 16 and 17, it is worth mentioning that the cytoskeleton is formed of solitary microtubules (Mts) and microfilaments (Mfs). The former is distributed along the anterior (ASS) and posterior subacrosomal spaces (PSS) and some Mts are observed in the outer side of the acrosomal cap and near the posterior nuclear shelf (PNS), in addition, some microfilaments appear in the subacrosomal cone. Moreover, the cytoskeleton in the posterior region of the nucleus showed longitudinal MMs, or solitary microtubules (Mts), in addition, numerous microfilaments that run in circular pathways to support the connections between the sperm head (SH) and caudal structures via the neck piece (NP) (Fig. 19 and 20).

It is not easy to conceive of any mechanism whereby the manchette microtubules disposed of parallel to one another and to the long axis of the nucleus could exert force perpendicular to their own axis. Yet, force in this direction would be required to produce the flattening of the sperm nucleus that is common to nearly all mammals.

3.2 Nuclear Shaping

Early spermatids have a round nucleus (N) filled with aggregations of fine chromatin granules (Chs), the surrounding cytoplasm illustrated numerous mitochondria (M), and few segments of RER, in addition, the presence of Golgi apparatus (G) starts to produce secretory vesicles (SVs) that will aggregate to form acrosome (Figs. 3-6). Figure 7 illustrates the distribution of cytoskeletal elements responsible for re-shaping of the nucleus. Later, a light comprehensive strength of cytoskeletal elements induced nuclear prolongation and formation of implantation fossa that appears in the ventrodorsal region at the posterior side of the nucleus (Figs. 5, 6). As the nuclear elongation proceeds, the fine chromatin granules aggregate and chromatin condensation begin (Figs. 8, 9).

In the next stage, when the posterior perinuclear space appears, the MMs and other cytoskeletal organelles, that surround it, generate compression strength to accelerate the nuclear prolongation towards the posterior direction (Fig. 10) and consequently to the anterior end (Figs. 11-13). The chromatin condensation proceeds then slow in parallel with the reduction of the perinuclear space. Thus, these thin-sections explain the relationship between nuclear elongation, the formation of perinuclear space and MMs strength. In the same time, the caudal ventral side of the nucleus is thickened to form a basal plate at which the posterior nuclear shelf appears (Fig. 12), while in Figure 13, the posterior ventromedial portion, the implantation fossa (IF) is formed to lodge the proximal centriole (PC) in the sperm neck (SN). However, there is a unique smaller space that appears on one side at the pre-equatorial plane (PeS). This space appears in conjunction with the elongation of the nucleus (Fig. 10) and disappears after the completion of chromatin condensation (Figs. 14). It has not been observed before in mammalian spermatids.

In late spermatids, the nuclear elongation and chromatin condensation are configured. At the present stage, the nucleus acquires a long conical shape with acute tip that end at the subacrosomal cone, filled with dense chromatin, and the presence of numerous nuclear canals (NCa). This new shape is supported by well-organized cytoskeletal structures that are distributed in the anterior (ASS) and posterior subacrosomal space (PSS), in addition, the microfilament in the subacrosomal cone (Figs. 16, 17).

Also worth mentioning, in the nucleus of the present spermatid, there are anterior and posterior nuclear shelves (Fig. 18) and unique implantation fossa (IF) at the posterior ventrodorsal side of the nucleus (Figs. 19 and 20).

3.3 Differentiation of acrosome

Fortunately, novel and complex structures are observed during the formation of the acrosome in the present spermatid as will be explained. The first sign of acrosomal formation is the activity of the Golgi apparatus (G), which secretes elements of the acrosome at the prospective anterior half of the nucleus in the form of acrosomal vesicle (AV) and acrosomal granule (AG) (Figs. 3, 4). Then, during nuclear elongation, both the acrosomal vesicle (AV) and granule (AG) spreads to occupy the upper half of the nuclear envelope and stop on at the nuclear shelf (NS) (Figs. 5-7).

In the next stage, after the beginning of nuclear elongation and chromatin condensation, the acrosomal granule appears as a dense large triangular acrosomal mass that will be differentiated into new described four regions. The former is a translucent terminal segment (TS) (Fig. 9), the remaining three portions appeared as a novel triangular acrosomal mass, which will be differentiated as shown in Figs. 10-13 into the crown (SC), anterior (AAS) and posterior acrosomal segments (PAS) at which a long acrosomal structure capping the anterior two-thirds of the nuclear envelope "anterior acrosomal cap "(AAC)" and separating from it by a narrow subacrosomal space (SAS) and a smaller subacrosomal cone (SC) (Fig. 13). Note that the acrosomal cap observed in Fig. 10, extends towards the posterior direction of the nucleus as anterior acrosomal cap (Figs. 11-13), which terminates at the equatorial region of the nucleus, which is called anterior nuclear shelf (ANS). Moreover, there is a novel triple branched structure, which is formed of a terminal dense rod (TDR) and two lateral dense arms (LDA) (Figs. 12, 13).

In late spermatid, as shown in the sagittal ultrathin section (Fig. 14), proved that the acrosomal cap differentiates into, a novel, long dorsal (DAC) and short ventral acrosomal cap (VAC), and consequently, both of them ends at the dorsal nuclear shelf (DNS) and a ventral one (VNS), respectively. Meanwhile, in the anterior longitudinal section, as shown in Fig. 15, the anterior and posterior acrosomal cap terminates at the anterior nuclear shelf (ANS) that appears at the lateral equatorial portions of the nucleus in parallel to the dorsal acrosomal cap (DAC) in the previous figure. From the above observations, the acrosomal cap covers about the anterior two-thirds of the nucleus (Figs. 14, 15) at the dorsal and both lateral sides, while less than half nuclear length of the nucleus at its ventral side (Fig. 14).

At this point, the anterior acrosomal cap swollen at its terminal ends as a posterior dense fusiform structure (PFE), and then, it extends towards the caudal nuclear region, forming posterior acrosomal cap (PAC) that destines at posterior nuclear shelf (PNS) forming small swallow fusiform caudal fusiform end (CFE) of the posterior acrosomal cap (PAC) (Figs. 15-18).

At this point, the anterior acrosomal cap swollen at its terminal ends as a posterior dense fusiform structure (PFE), and then, it extends towards the caudal nuclear region, forming posterior acrosomal cap (PAC) that destines at posterior nuclear shelf (PNS) forming small swallow fusiform caudal fusiform end (CFE) of the posterior acrosomal cap (PAC) (Figs. 16-18).

Moreover, the crown segment (CS) appears as club-shaped, which is surrounded by crown dense diadems (CDD) that imprecate along the anterior acrosomal cap as a chain of dense diadems (ChD) (Fig. 18).

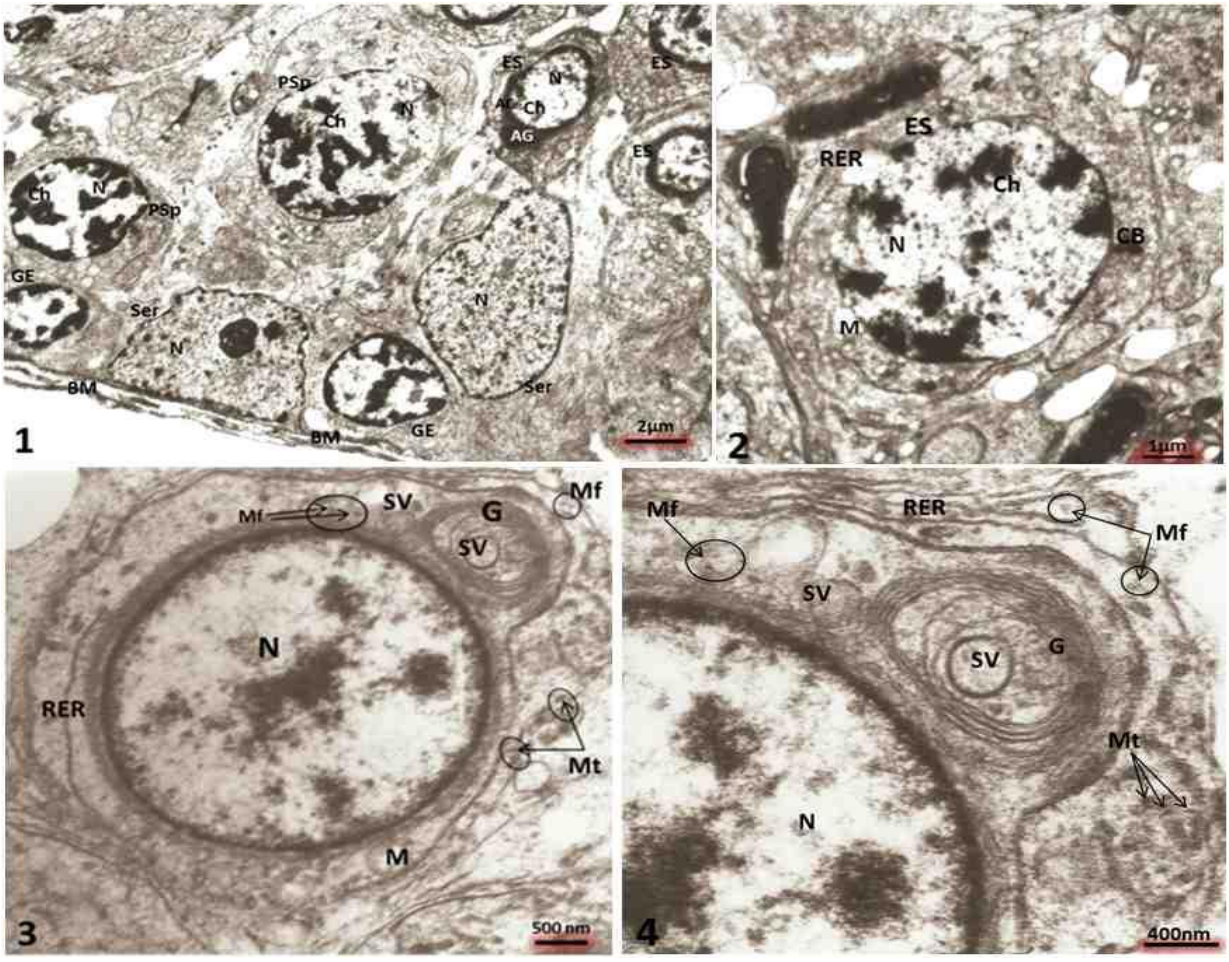

Fig. 1. Electron micrograph showed epithelium of a seminiferous tubule. Note that germinal epithelium (GE) and Sertoli cells (Ser) are situated on a special basement membrane (BM), while other spermatogenic cells can be seen. Primary spermatocytes (PSp) contain large nucleus (N) with accumulating chromatin (Ch), early spermatids (ES) has small nucleus with fine chromatin granules and their anterior side capping with an acrosomal granule (AG) and acrosomal vesicle (AV). Bar: 2µm, X 3000. **Fig. 2.** Electron micrograph showed early spermatid contains round nucleus (N) filled with aggregations of fine chromatin granules (Ch), the cytoplasm illustrated numerous mitochondria (M), and few segments of RER. Bar: 1µm, X 2000. **Fig. 3.** Electron micrograph showed active spermatid in which Golgi apparatus (G) starts to produce secretory vesicles (SV) that will be aggregated to form acrosome. Bar: 500nm, X 10000. **Fig. 4.** Magnified portion from figure 3 showed rough endoplasmic reticulum (RER), units of numerous microtubules (Mt) and microfilaments (Mf) that run in circular patterns. Bar: 400nm, X 20000.

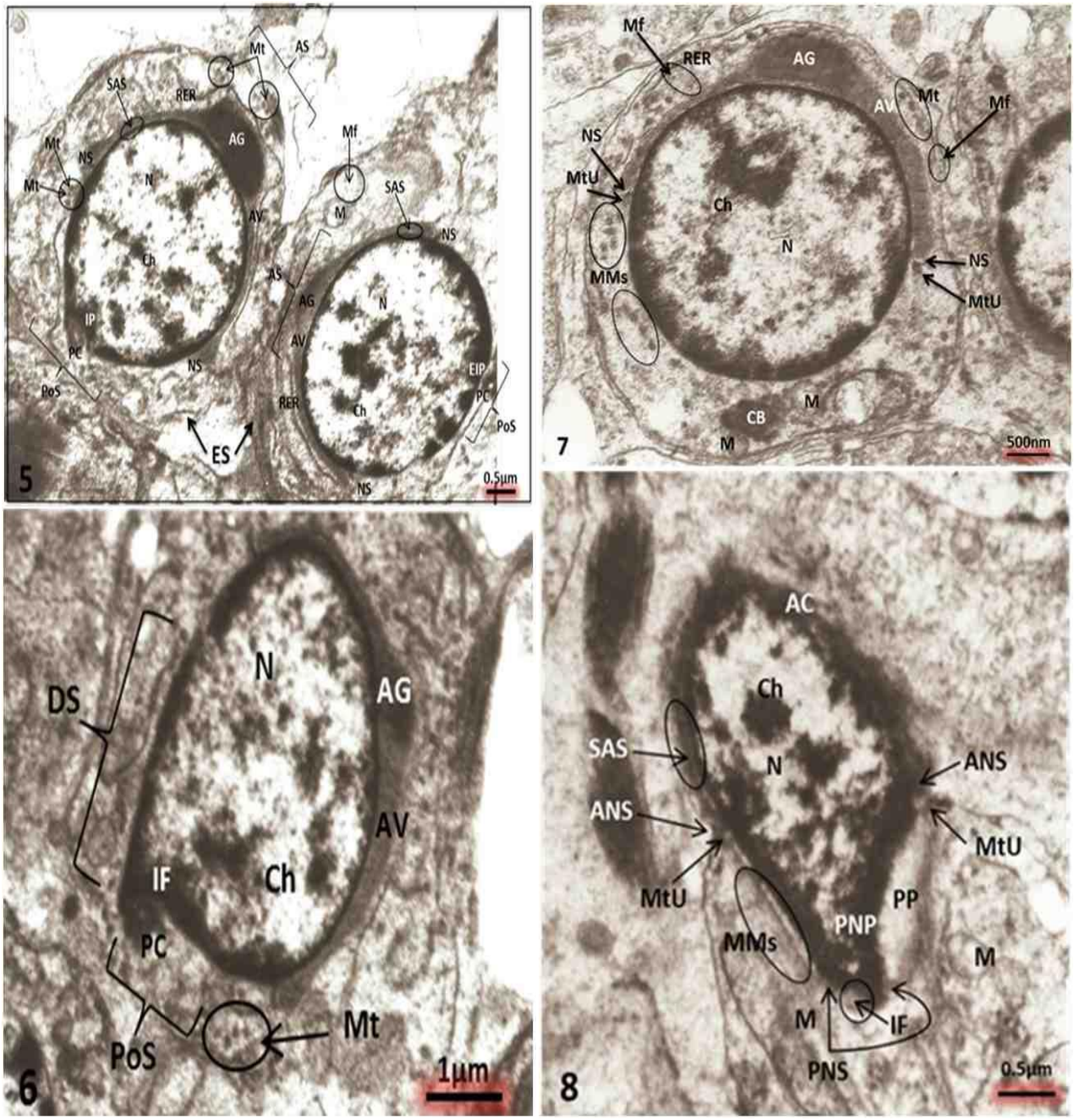

Fig. 5. Electron micrograph showed two stages of active spermatids (ES). Right: shallow and early implantation fossa (EIP) formed in the posterior side of the nucleus (PoS) in which proximal centriole will be enclosed. The anterior side of the nucleus (AS) showed early acrosomal granule and acrosomal cap surrounds its anterior half and stop on a region at the equatorial level, nuclear shelf (NS) and separated from the nuclear envelope by a narrow subacrosomal space (SAS). Left: Active spermatids represent a later stage next to that observed in the right. Note deeper implantation fossa (IP) at the posterior side of the nucleus (PoS), larger acrosomal granule (AG), acrosomal vesicle (AV), long segments of RER and numerous microtubules run in circular patterns (Mt). Bar 0.5µm. X 7500. **Fig. 6.** Electron micrographs showed that the proximal centriole (PC) is situated inside the implantation fossa (IF) that appears at the posterior ventrodorsal side of the nucleus. Bar 1µm. X 4000. **Fig. 7.** Electron micrograph of early spermatid just before nuclear elongation showed the formation of large unit of microtubule (MtU) that appears at the nuclear shelf (NS), in addition, numerous solitary microtubules run in a circular direction to surround the upper nuclear portion (Mt), its equatorial and sub-equatorial half of the nucleus that appears to surround the nucleus and run in circular pathways (MMs). These Manchette microtubules will be re-orienting into longitudinal direction as shown in figures 8-13 in order to nuclear re-shaping. Bar: 500nm, X 10000. **Fig. 8.** Electron micrographs showed the formation of acrosomal cap (AC), subacrosomal space (SAS), anterior (ANP) and posterior nuclear protrusion (PNP), chromatin condensation, the presence of anterior (ANS) and posterior nuclear shelf ((PNS) at juxta-equatorial region, and implantation fossa (IF) at the posterior side of the nucleus, where the MMs are run parallel to its long axis and attach to both the MtU at the anterior (ANS) and posterior nuclear shelves (PNS), in addition, the presence of the posterior perinuclear space (PP) along one side of the posterior edge of the nucleus. Note the migration of cellular organelles at the posterior direction of the nucleus. M: Mitochondria. Bar 0.5µm.

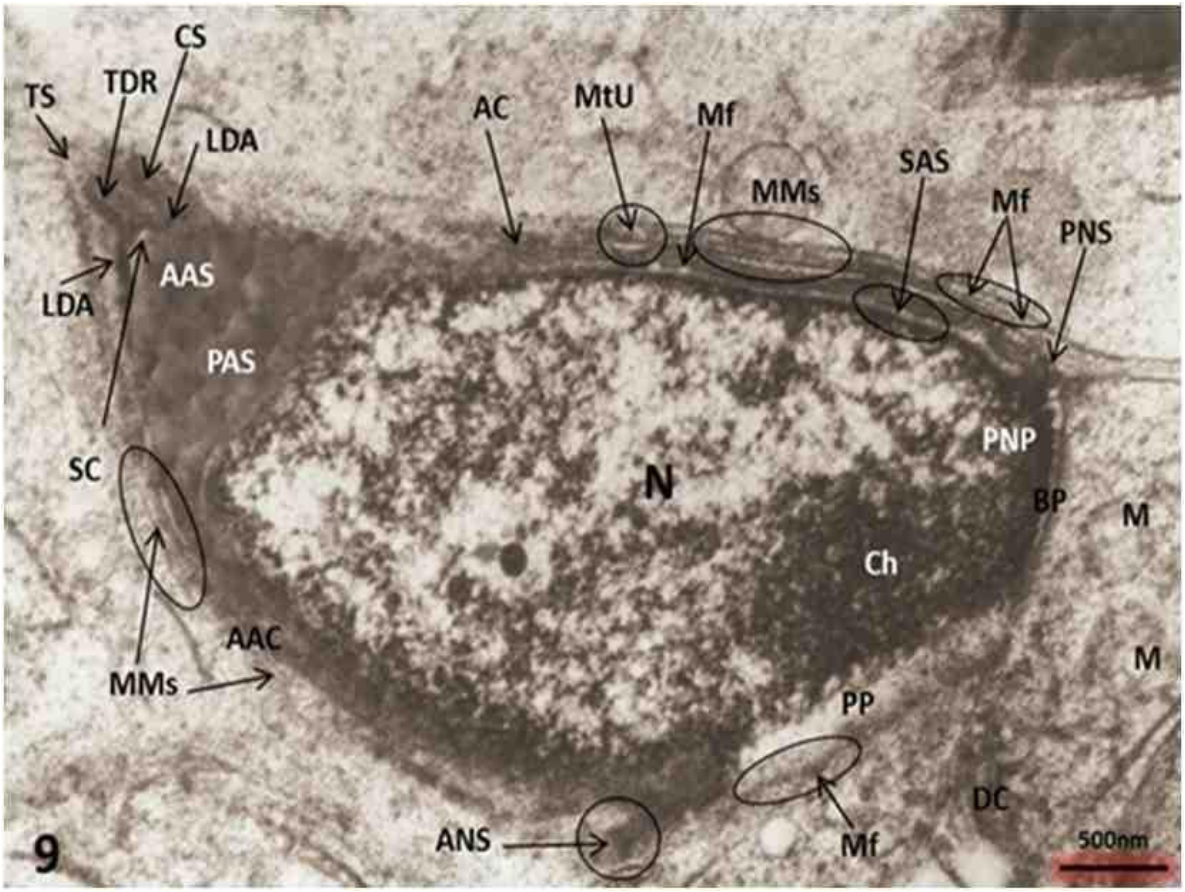

Fig. 9. Electron micrographs showed that the acrosome starts to differentiate into four regions that are considered as new subdivisions in the acrosome. The former is a translucent terminal segment (TS), the remaining three portions appeared as a novel triangular acro somal mass, which will be differentiates into the crown (SC), anterior (AAS) and posterior acrosomal segments (PAS) at which a long acrosomal structure capping the anterior two-third of the nuclear envelope "anterior acrosomal cap "(AAC)" and separating from it by a narrow subacrosomal space (SAS) as observed in figure 12. Moreover, there is a novel triple branched structure, which is formed of a terminal dense rod (TDR) and two lateral dense arms (LDA). Also, this figure clarifies the re-orientation of MMs and Mf into longitudinal or circular directions to surround the posterior half of the nucleus and the posterior perinuclear space (PP) that appears in the ventral side of the posterior nuclear protrusion (PNP), in addition, the presence of anterior (ANS) and posterior nuclear shelves (PNS), basal plate (BP). Note that the chromatin granules (Ch) are condensed at the peripheries of the nuclear envelope, the distal centriole (DC) is situated near the posterior ventrolateral side of the nucleus, and the presence of few mitochondria (M). Bar: 500nm, X 12000.

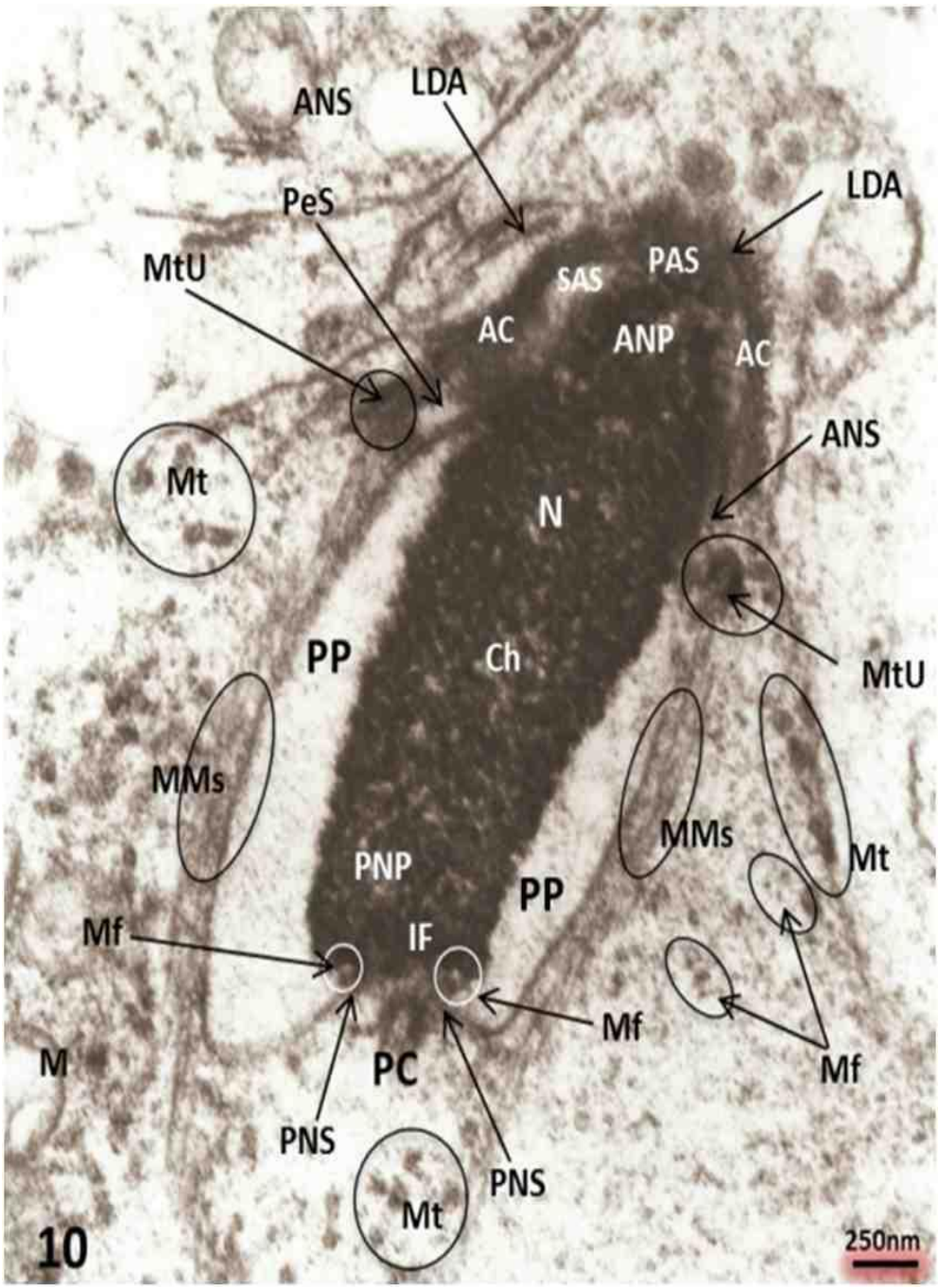

Fig. 10. Electron micrograph showed successive nuclear elongation towards the anterior (ANP) and posterior sides of the nucleus (PNP), chromatin (Ch) condensation markedly increases, the perinuclear space expands to surround the posterior two-third of the elongated nucleus. This space is bounded between the anterior (ANS) and posterior nuclear shelves (PNS). Also, there is a new smaller space appe ars on one side at juxta-equatorial nuclear region, pre-equatorial space (PeS). Moreover, the cytoskeleton is formed of MtU, MMs, in addition, solitary Mt and Mf appear to organize the nuclear elongation, the formation of the implantation fossa (IF). The MMs attach to the MtU at the equatorial region posterior to the anterior (ANS) and posterior nuclear shelves (PNS). The MMs still generate a compressive strength on the pos terior perinuclear space (PP) causing more nuclear prolongation. Some microfilaments (Mf) appear at posterior end of the nucleus that may be involved in the formation of the implantation fossa (IF). Other cytoskeletal elements are distributed in the posterior regions of the develop ing spermatid. Note that the proximal centriole (PC) in enclosed in the implantation fossa (IF). As regards the acrosomal regions, the present thin-section showed the lateral dense arm (LDA), posterior acrosomal segment (PAS), and the acrosomal cap (AC). Bar: 500nm, X 15000.

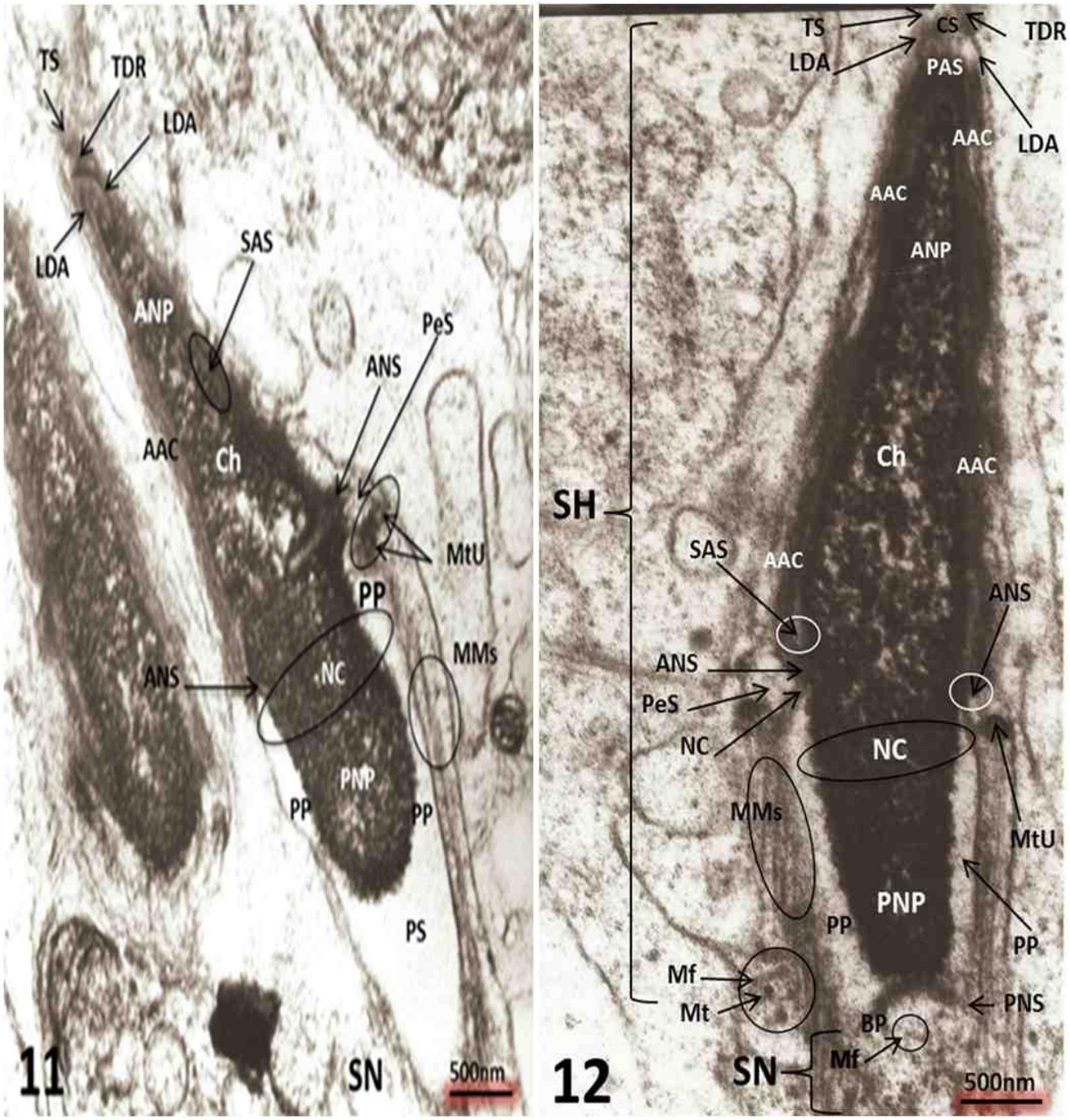

Fig. 11. Electron micrographs showed that the compressive strength on the posterior perinuclear space (PP) causing nuclear constriction (NC) and increase the anterior (ANP) and posterior nuclear prolongation (PNP), the ANP is covered by an anterior acrosomal cap (AAC) and separated from it by a narrow subacrosomal space (SAS). The triple branched structure of the acrosome appears including the terminal dense rod (TDR), and two lateral dense arms (LDA). In the present spermatid, the posterior side of the nucleus showed posterior space (PS) that fused with the posterior perinuclear space (PP), both of them are supported with longitudinal MMs that attach to the large units of microtubule (MtU) and run posteriorly to the connecting piece in the sperm neck (SN). Note that the presence of pre-equatorial space as its seen in the previous stage. Bar: 500nm, X 12000**. Fig. 12.** Electron micrograph showed an advanced stage of spermatid with three different regions of acrosomal segments, anterior (ANP) and posterior nuclear elongation (PNP), chromatin condensation and nuclear constriction (NC). The precursor portions of the acrosome explained in figure 9 are differentiated in the present stage, into crown, anterior, posterior acrosomal segments (PAS) that attach with the anterior acrosomal cap (AAC), which extends to the anterior nuclear shelf (ANS). The later is separated from the tip of the conical nuclear prolongation by a narrow subacrosomal space (SAS). In the terminal segment, there is a triple structure that formed of terminal dense rod (TDR), and two lateral dense arms (LDA). Moreover, more solitary microtubules appear at the posterior end of the nucleus. They arranged in a circular pathway at the posterior end of the nucleus to support the attachment between sperm head (SH) and neck (SN). Note that the presence of pre-equatorial space (Pes) and posterior perinuclear space (PP). Concerning with the cytoskeleton, the described elements (Mt and Mf), of the previous stage, control the migration of subcellular organelles towards the posterior end of the present spermatid at the sperm neck (SN). Bar: 500nm, X 12000**.**

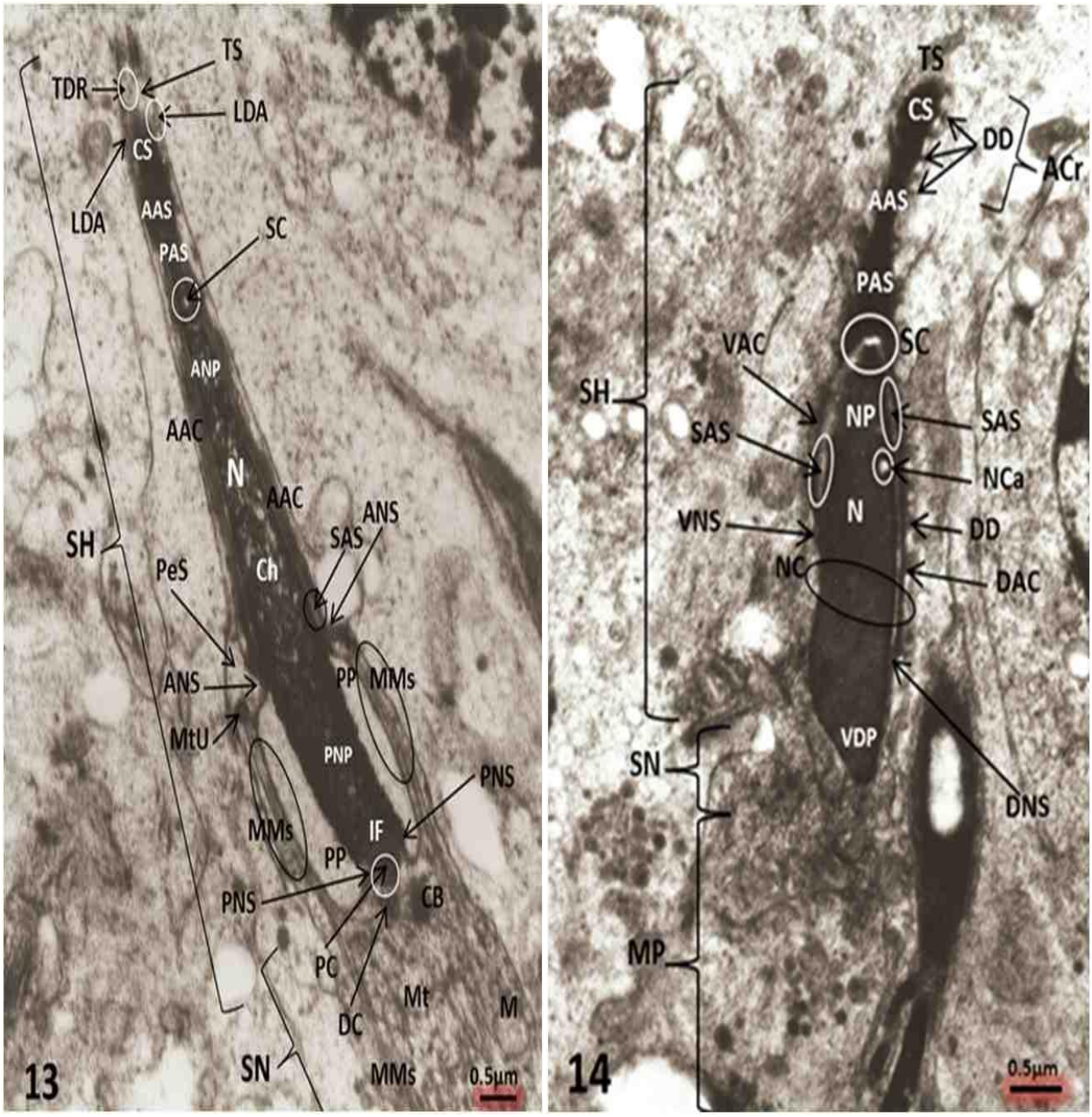

Fig. 13. Electron micrograph showed continuous chromatin condensation and nuclear prolongation to the anterior (ANP) and posterior (PNP) directions. The space of this cone is in a direct attachment with the subacrosomal space (SAS) on both sides. Also, the PAS is attached with a long anterior acrosomal cap (AAC) that capping the anterior conical protrusion of the nucleus and this cap extends along the two-third of the nucleus then terminates at the anterior nuclear shelf (ANS) at the equatorial level of the sperm head. At this point, there is a small pre-equatorial space (PeS) that appears on one side at juxta-nuclear region. In addition to the MMs, the cytoskeleton in the present stage showed other solitary microtubules that are situated in the posterior side of the nucleus, where they are arranged in longitudinal and transverse directions for tight attachment between head (SH) and neck (SN) of the developing sperm. However, this stage proved that the posterior perinuclear space starts to be decreased and consequently, the nuclear prolongation is continued in a slow rate, meanwhile, the chromatin condensation will be continued in the next stages. The posterior end of the nucleus illustrates the presence of implantation fossa (IF) that lodge the proximal centriole (PC) and the connecting piece in the sperm neck (SN) showed some organelles that include the distal centriole (DC) situated in the implantation fossa (IF), chromatoid body (CB), MMs, solitary microtubules (Mt) that run in longitudinal and transverse directions, mitochondrion (M). Bar: 0.5µm, X 7500. **Fig. 14.** Electron micrograph showed sagittal section that clarifies the developing sperm head (SH), neck (SN) and middle piece (MP). This stage is the most important because it is clarified that chromatin condensation ends, the ventral acrosomal cap (VAC) is shorter than the dorsal one (DAC) and both of them stopped at the ventral (VNS) and dorsal nuclear shelves (DNS), respectively. Note the presence of nuclear constriction (NC) and nuclear canal (NCa), posterior ventrodorsal protrusion of the nucleus (VDP) that previously described in figure 6, the other portions of the acrosome can be observed, which include terminal (TS), crown (CS), anterior (AAS) and posterior acrosomal segments (PAS), subacrosomal cone (SC), subacrosomal space (SAS). The crown segment gives an acrosomal crown (ACr) that formed a thin chain of dense diadems (DD) which surround the crown segment and extend along the dorsal acrosomal cap (DAC). Bar: 0.5µm, X 6000.

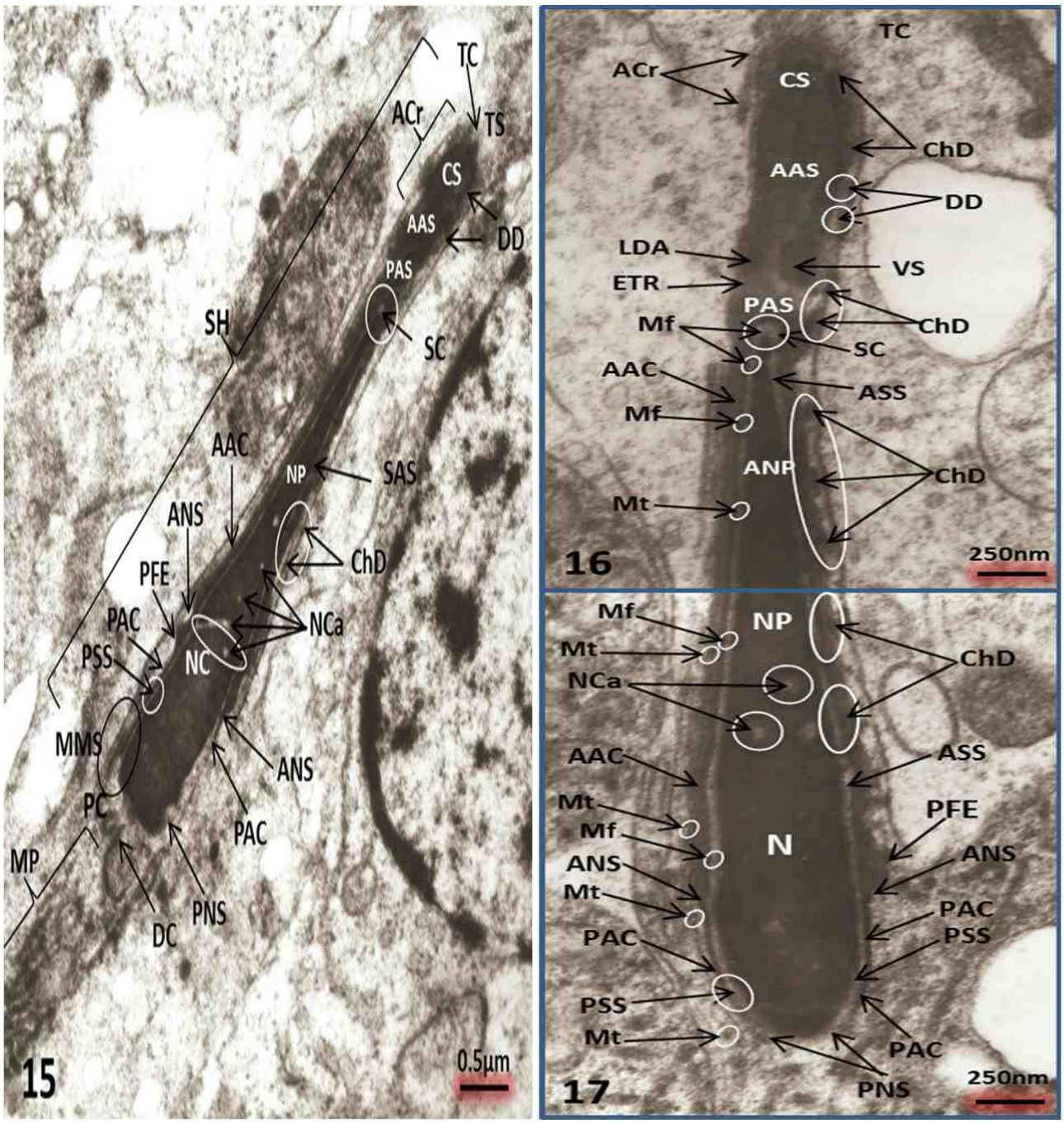

Fig. 15. Electron micrograph showed anterior longitudinal section of late spermatid. This ultrathin section gives us a complementary imagination about new structures that appeared on both rights and left sides of this spermatid and numerous nuclear canals (NCa) that appear in the middle region of the nucleus after completion of chromatin condensation. The present stage proved that the crown segment gives acrosomal crown (ACr) that covered with a thin chain (ChD) formed of numerous small dense diadems (DD) which surround the crown segment and extend posteriorly along the anterior acrosomal cap (AAC) that ends at the anterior nuclear shelf (ANS). Moreover, additional posterior acrosomal cap originates at the anterior nuclear shelf and extends posteriorly as a thin layer to the posterior nuclear shelf (PNS). Hence, the acrosomal cap differentiates into a long anterior (AAC) and short posterior acrosomal cap (PAC) that separated from the posterior region of the nuclear envelope by a narrow space called posterior subacrosomal spaces (PSS). Bar: 0.5µm, X 7500**. Figs. 16 & 17.** Two reconstructed electron micrograph showed anterior longitudinal section in very late spermatid. This stage illustrated that both lateral dense arms (LDA) are developed, capping both the crown (CS) and anterior segments of the acrosome (AAS), while the posterior acrosomal segment is separated from the anterior one by an electron translucent region (ETR), in addition, the posterior acrosomal cap (PAC) complete its trip to most posterior end of the nucleus at the posterior nuclear shelf (PNS) and separating from the nucleus by additional narrow space called posterior subacrosomal space (PSS). Worth mentioning, the cytoskeleton in the present stage is formed of solitary microtubules (Mts) and microfilaments (Mf). The former is distributed along the anterior and posterior subacrosomal spaces and some Mts are observed on the outer side of the acrosomal cap and near the posterior nuclear shelf. Bar: 250nm, X 15000**.**

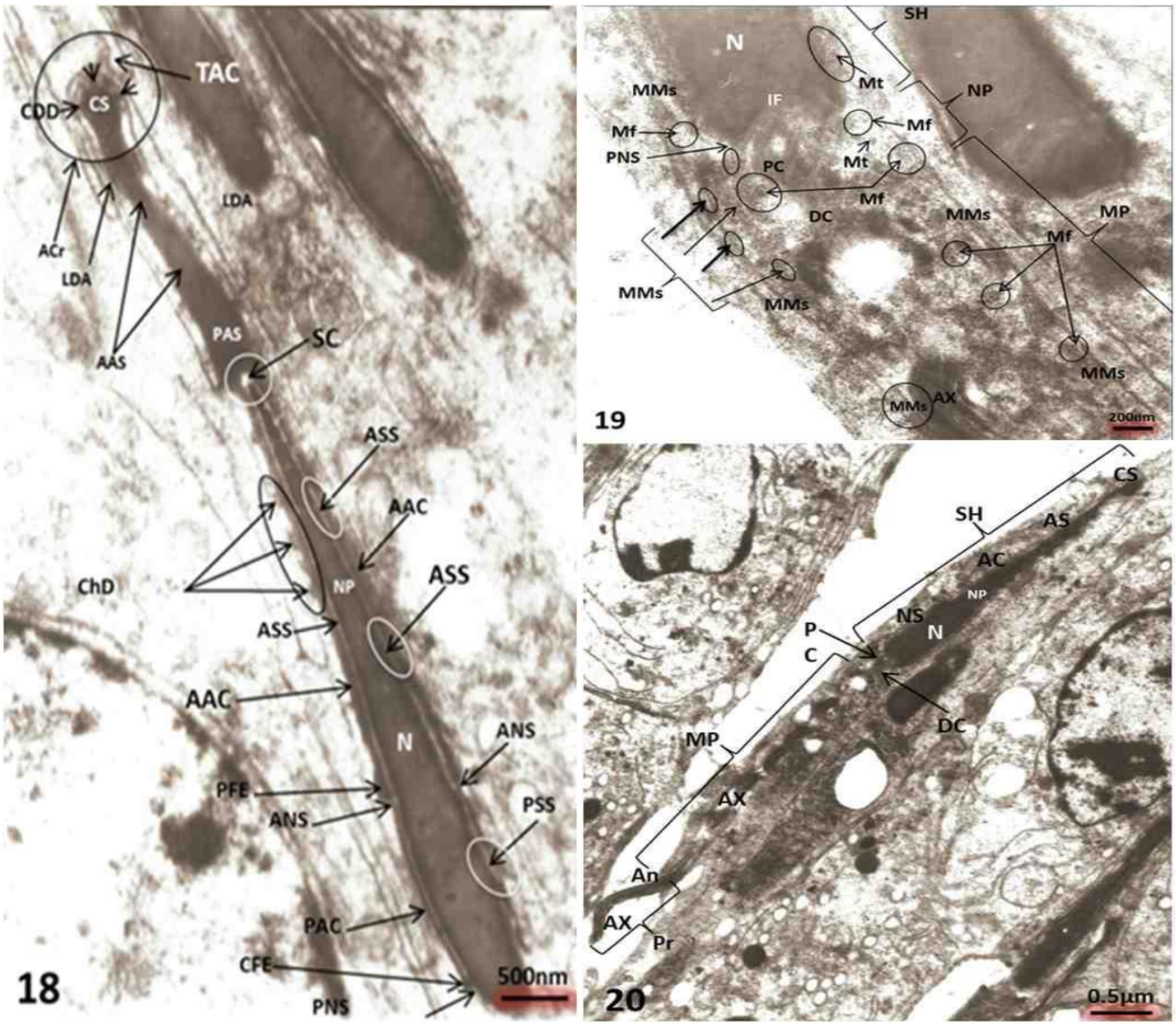

Fig. 18. Electron micrograph showed three advanced stages of late spermatids. This stage gives us the final configuration of the different acrosomal regions. The crown segment (CS) takes club-shape, which is surrounded by Crown dense diadems (CDD) that imprecate along the anterior acrosomal cap as a chain of dense diadems (ChD). The anterior acrosomal segment (AAS) have trapezoid shape and fused with the posterior acrosomal segment (PAS) as a dense region, the caudal end of the anterior acrosomal cap enlarges as fusiform structure (PFE) at the anterior nuclear shelf (ANS), also the posterior acrosomal cap (PAC) terminates as smaller fusiform structure (CFE) at the posterior nuclear shelf (PNS). The subacrosomal spaces include subacrosomal cone at the tip of the nuclear prolongation, Anterior (ASS) and posterior subacrosomal spaces (PSS). Bar: 0.5µm, X 7500**. Fig. 19.** Electron micrograph showed longitudinal section in late spermatid through the sperm head, neck, and middle piece. This stage illustrated the structures that appeared at the posterior end of the nucleus. Note that the implantation fossa lodges the proximal centriole and the distal one is situated perpendicular to it. Elements of cytoskeleton consist of longitudinal MMs, or solitary microtubules, in addition, numerous microfilaments that run in circular pathways to support the connections between the sperm head and caudal structures. Bar: 500nm, X 10000**. Fig. 20.** Low magnification electron micrograph showed developed spermatid. The sperm head (SH) provided with acrosome, elongated nucleus that ends at the nuclear fossa (IF), neck region include the both the proximal (PC) and distal centriole (DC), the middle piece include the axial filament (AX) surrounded by mitochondrial sheath, the principal piece appears posterior to the end of the middle piece (MP) at the annulus (An). Bar: 0.5µm, X 3000**.**

4. Discussion

Present results describe the stages that will help us to conceive the mechanism in which MMs control the nuclear elongation, formation of the implantation fossa at which the connecting piece of the tail formed. Also, the MMs and microfilaments re-orient their direction in the anterior and posterior halves of the nucleus, in parallel to its long axis and/or to horizontally surround the posterior nuclear region.

Similar longitudinal MMs reported, just behind the distal extremity of the acrosomal cap in bat spermatids [40]. In mice spermatids, a cone-shaped bundle of MMs encases the nuclear posterior pole [10]. However, longitudinal and circular bundles of MMs are described in marsupial spermatids [41].

Also, the Manchette was described in mammalian spermatids as a transient sleeve-like organelle that appears as longitudinal microtubular elements, displaced laterally parallel to the long axis of the spermatid during early spermiogenesis, encircling the caudal pole of the nucleus, and then extending back to connect the sperm head with neck region [8,9,10,26]. However, Fouquet *et al.*, [11] follow the localization of dynactin complex, associated with dynein of microtubules. They concluded that in round spermatid it appears near the centrosome and at the Golgi apparatus, and in elongated spermatids, it was arranged along microtubules of the manchette and at their attachment sites to the nuclear envelope, while disappeared in the testicular spermatozoa. They added that the various localizations of the dynactin might contribute to the activities of the centrosome and of the Golgi apparatus, as well as the shaping of the nucleus by MMs.

The present author believes that the solitary microtubules observed in round spermatid depolymerized then repolymerized in longitudinal and circular bundles tangential to the caudal half of the nucleus. These bundles may generate intrinsic compression strength perpendicular to their long axis induced nuclear prolongation. It is worth mentioning that, the generated strength is gently forced the perinuclear space that surrounds the posterior half of the nucleus to accelerate the anterior and posterior nuclear elongation without disturbing the chromatin condensation.

The Manchette acts as a track for the transport of cellular components between the nucleus and distal cytoplasmic regions of the elongating spermatid [12,37,42].

Present results showed the formation of oval or rounded acrosomal granule and a thin layer of acrosomal vesicle that capping at the anterior proximity of the nucleus. The former develops into novel acrosomal structures include crown, anterior and posterior segments that extend posteriorly to capping two-thirds of the nuclear envelope. Similar, acrosomal vesicle was described in the early spermatid of the musk shrew [44,45], marmoset monkey [6,7,28], also, a membrane-bounded acrosomal granule in New Zealand white rabbits [43]. However, several proacrosomal vesicles were observed in marsupial and bat early spermatids [40,41]. These acrosomal vesicles became flattened and extend to form an acrosomal cap [6,7,28,40,41,43,45] that oriented in a longitudinal direction and capping the elongated nuclei. In the marsupials, the acrosomal cap is re-oriented to the horizontal plane and protrudes as a projecting U-shape [41], while in the musk shrew, a flat fan-like acrosome appears in the late spermatid [44,45].

On the other hand, a new triple acrosomal structure is observed in the present spermatid that formed of anterior acrosomal rod and two short lateral acrosomal arms, such structures are not described in mammalian spermatids before. In addition, the club-shaped crown segment is surrounded by an imprecated chain of dense diadems that extends along the anterior acrosomal cap. Such structures could be specific for the present species, hence it is not observed, yet, in other rodents.

As regards to the posterior nuclear shelf appeared after the formation of the anterior one. Most publications described only one acrosomal shelf as a ring structure at the posterior end of the nucleus of the developing spermatids of rabbits, mice, monkeys, bats and in fat-tailed jerbil, *P. duprasi* [11,37,40,43].

5. Conclusion

From the present study, it is strongly concluded that the differentiation of sperm head of lesser Egyptian jerboa, *Jaculus jaculus* is controlled by cytoskeletal elements, especially manchette microtubules which master the shaping of the spermatid nucleus during its successive development. Present results showed the formation of oval or rounded acrosomal granule and a thin layer of acrosomal vesicle that capping at the anterior proximity of the nucleus. The former develops into novel acrosomal structures include crown, anterior and posterior segments that extend posteriorly to capping two-thirds of the nuclear envelope. A new triple acrosomal structure is observed in the present spermatid that formed of anterior acrosomal rod and two short lateral acrosomal arms, such structures are not described in mammalian spermatids before. In addition, the club-shaped crown segment is surrounded by an imprecated chain of dense diadems that extends along the anterior acrosomal cap. Such structures could be specific for the present species, hence it is not observed, yet, in other rodents.

It is worth mentioning that a new translucent perinuclear space appears at the posterior end of the nucleus. It receives a gently generated compression induced by the cytoskeletal elements to produce the anterior and posterior nuclear elongation and to protect DNA during nuclear condensation.

References

[1]. Amann, R.P. (2008). The cycle of the seminiferous epithelium in humans: a need to revisit? *Journal of Andrology*, 29(5): 469-487.

[2]. Jeong, S.J., Yoo, J. and Jeong, M.J. (2004). Ultrastructure of the abnormal head of the epididymal spermatozoa in the big white-toothed shrew, *Crocidura lasiura*. *Korean J. Electron Microscopy*, 34(3): 179-184.

[3]. Tang, X.M., Lalli, M.F. and Clermont, Y. (1982). A cytochemical study of the Golgi apparatus of the spermatid during spermiogenesis in the rat. *Am. J. Anat.*, 163: 283-294.

[4]. Burgos, M.H. and Gutierrez, L.S. (1986). The Golgi complex of the early spermatid in guinea pig. *Anat. Rec.*, 216: 139-145.

[5]. Ho, H.C., Tang, C.Y. and Suarez, S.S. (1999). Three-dimensional structure of the Golgi apparatus in mouse spermatids: a scanning electron microscopic study. *Anat. Rec.*, 256: 189-194.

[6]. Moreno, R.D., Ramalho-Santos, J., Chan, E.K., Wessel, G.M. and Schatten, G. (2000a). The Golgi apparatus segregates from the lysosomal/acrosomal vesicle during rhesus spermiogenesis: structural alterations. Dev. Biol., 219: 334- 349.

[7]. Moreno, R.D., Ramalho-Santos, J., Sutovsky, P., Chan, E.K.L. and Schatten, G. (2000b). Vesicular traffic and Golgi apparatus dynamics during mammalian spermatogenesis: Implications for acrosome architecture. *Biol. Reprod.*, 63: 89-98.

[8]. Rattner, J.B. and Brinkley, B.R. (1972). Ultrastructure of mammalian spermiogenesis. 3. The organization and morphogenesis of the manchette during rodent spermiogenesis. *J. Ultrastruct. Res.*, 41(3): 209-18.

[9]. Meistrich, M.L., Trostle-Weige, P.K., Russell, L.D. (1990). Abnormal manchette development in spermatids of azh/azh mutant mice. *Am. J. Anat.*, 188(1): 74-86.

[10]. Russell, L.D., Russell, J.A., MacGregor, G.R., Meistrich, M.L. (1991). Linkage of manchette microtubules to the nuclear envelope and observations of the role of the manchette in nuclear shaping during spermiogenesis in rodents. *Am. J. Anat.*, 192: 97-120.

[11]. Fouquet, J., Kann, M., Soues, S. and Melki, R. (2000). ARP1 in Golgi organisation and attachment of manchette microtubules to the nucleus during mammalian spermatogenesis. *J. Cell Sci.*, 113: 877-886.

[12]. Kierszenbaum, A.L. (2002). Intramanchette transport (IMT): Managing the making of the spermatid head, centrosome, and tail. *Mol. Reprod. Dev.*, 63(1): 1-4.

[13]. Yokota, S. (2008). Historical survey on chromatoid body research. *Acta Histochem. Cytochem.*, 41(4): 65-82.

[14]. Jin, Q.S., Kamata, M., Garcia del Saz, E. and Seguchi, H. (1995). Ultracytochemical study of trimetaphosphatase activity during acrosomal formation in the mouse testis. *Histol. Histopathol.*, 10: 681-689.

[15]. Sapsford, C.S., Rae, C.A. and Cleland, K.W. (1970). Ultrastructural studies on the development and form of the principal piece sheath of the bandicoot spermatozoon. *Aust. J. Zool.*, 18: 21-48.

[16]. Oko, R. and Clermont, Y. (1989). Light microscopic immunocytochemical study of fibrous sheath and outer dense fiber formation in the rat spermatid. *Anat. Rec.*, 225: 46-55.

[17]. Kim, Y.H., de Kretser, D.M., Temple-Smith, P.D., Hearn, M.T., McFarlane, J.R. (1997). Isolation and characterization of human and rabbit sperm tail fibrous sheath. *Mol. Hum. Reprod.*, 3(4): 307-313.

[18]. Rawe, V.Y., Galaverna, G.D., Acosta, A.A., Olmedo, S.B., Chemes, H.E. (2001). Incidence of tail structure distortions associated with dysplasia of the fibrous sheath in human spermatozoa. *Hum. Reprod.*, 16(5):879-86.

[19]. Eddy, E.M., Toshimori, K. and O'Brien, D.A. (2003). Fibrous sheath of mammalian spermatozoa. *Microsc. Res. Tech.*, 61: 103-115.

[20]. Ricci, M. and Breed, W.G. (2005). Morphogenesis of the fibrous sheath in the marsupial spermatozoon. *J. Anat.*, 207(2): 155-164.

[21]. Guan, J., Kinoshita, M. and Yuan, L. (2009). Spatiotemporal Association of DNAJB13 with the annulus during mouse sperm flagellum development. *BMC Dev. Biol.*, 9: 23. doi: 10.1186/1471-213X-9-23.

[22]. Dadoune, J.P. and Alfonsi, M.F. (1986). Ultrastructural and cytochemical changes of the head components of human spermatids and spermatozoa. *Gamete Res.*, 14: 33-46.

[23]. Toyama, Y., Iwamoto, T., Yajima, M., Baba, K. and Yuasa, S. (2000). Decapitated and decaudated spermatozoa in man, and pathogenesis based on the ultrastructure. *Int. J. Androl.*, 23(2): 109-115.

[24]. Burgos, M.H. and Fawcett, D.W. (1955). Studies on the fine structure of the mammalian testis. I. Differentiation of the spermatid in the cat (*Felis domestica*). *J. Biophys. Biochem. Cytol.*, 25;1(4):287-300.

[25]. Sapsford, C.S., Rae, C.A., Cleland, K.W. (1969). Ultrastructual studies on maturing spermatids and on sertoli cells in the bandicoot *Perameles nasuts* Geoffroy (Marsupialia). *Australian Journal of Zoology*, 17: 195-292.

[26]. Fawcett, D.W., Anderson, W.A. and Phillips, D.M. (1971). Morphogenetic factors influencing the shape of the sperm head. *Developmental Biology*, 26(2): 220-251.

[27]. Singwi, M.S. and Lall, S.B. (1983). Spermatogenesis in the non-scrotal bat-*Rhinopoma kinneari* Wroughton (Microchiroptera: Mammalia). *Acta Anat. (Basel)*, 116(2): 136-145.

[28]. Holt, W.V. and Moore, H.D. (1984). Ultrastructural aspects of spermatogenesis in the common marmoset (*Callithrix jacchus*). *J. Anat.*, 138: 175-188.

[29]. Mori, T., Arai, S., Shiraishi, S. and Uchida, T.A. (1991). Ultrastructural Observations on Spermatozoa of the Soricidae, with Special Attention to a Subfamily Revision of the Japanese Water Shrew *Chimarrogale himalayica*. *J. Mamm. Soc. Japan*, 16: 1-12.

[30]. Lin, M. and Jones, R.C. (2000). Spermiogenesis and spermiation in a monotreme mammal, the platypus, Ornithorhynchus anatinus. *Journal of Anatomy*, 196(2): 217-232.

[31]. Jeong, S.J., Park, J.C., Kim, H.J., Bae, C.S., Yoon, M.H., Lim, D.S., Jeong, M.J. (2006). Comparative fine structure of the epididymal spermatozoa from three Korean shrews with considerations on their phylogenetic relationships. *Biocell*, 30(2): 279-286.

[32]. Challice, C.E. (1953). Electron microscope studies of spermiogenesis in some rodents. *J. R. Microsc. Soc.*, 73(3): 115-27.

[33]. Minamino, T. (1955). Spermiogenesis in the albino rat as revealed by electron microscopy. *Electron Microsc.*, 4: 249-253.

[34]. Pelletier, R.M. and Friend, D.S. (1983). Development of membrane differentiations in the guinea pig spermatid during spermiogenesis. *Am. J. Anat.*, 167: 119-141.

[35]. Lim, S.L., Qu, Z.P., Kortschak, R.D., Lawrence, D.M., Geoghegan, J., Hempfling, A.L., Bergmann, M., Goodnow, C.C., Ormandy, C.J., Wong, L., Mann, J., Scott, H.S., Jamsai, D., Adelson, D.L., O'Bryan, M.K. (2015). HENMT1 and piRNA Stability Are Required for Adult Male Germ Cell Transposon Repression and to Define the Spermatogenic Program in the Mouse. *PLoS Genet*., 11(10): e1005620. doi: 10.1371/journal.pgen.1005620.

[36]. Shahin, A.A.B. and Ibraheem, M.H. (1998). Sperm morphology of the dipodid rodents (Jerboas) common in Egypt. *Belgian Journal of Zoology*, 128(2): 189-200.

[37]. Sarhan, O.M.M. (2009). Spermiogenesis of Egyptian mammals: 1-Sperm head and tail differentiation of fat-tailed gerbil *Pachyuromys duprasi*. *Egypt. J. Zool*., 53: 283-309.

[38]. Sarhan, O.M. and Hefny, H.A. (2016). Ultra-differentiation of sperm tail of Lesser Egyptian Jerboa, *Jaculus jaculus* (Family: Dipodidae). *J. Adv. Lab. Res. Biol.*, 7(1), 27-35.

[39]. IUCN (International Union for Conservation of Nature, 2015). *Jaculus jaculus*. In: IUCN 2015. The IUCN Red List of Threatened Species. Version 2015.2. http://www.iucnredlist.org. Downloaded on 14 July 2015.

[40]. Jung-Hun, L. (2003). Cell Differentiation and Ultrastructure of the Seminiferous Epithelium in Myotis macrodactylus. *Korean Journal of Electron Microscopy*, 33(1): 25-39.

[41]. Lin, M., Harman, A. and Rodger, J.C. (1997). Spermiogenesis and spermiation in a marsupial, the tammar wallaby (*Macropus eugenii*). *J. Anat.*, 190: 377-395.

[42]. Tovich, P.R., Sutovsky, P. and Oko, R.J. (2004). Novel aspect of perinuclear theca assembly revealed by immunolocalization of non-nuclear somatic histones during bovine spermiogenesis. *Biol. Reprod.*, 71(4):1182-94.

[43]. Bedford, J.M. and Nicander, L. (1971). Ultrastructural changes in the acrosome and sperm membranes during maturation of spermatozoa in the testis and epididymis of the rabbit and monkey. *J. Anat.*, 108: 527-543.

[44]. Kurohmaru, M., Kobayashi, H., Hattori, S., Nishida, T. and Hayashi, Y. (1994). Spermatogenesis and ultrastructure of a peculiar acrosomal formation in the musk shrew, *Suncus murinus*. *J. Anat*., 185(3): 503-509.

[45]. Kurohmaru, M., Maeda, S., Suda, A., Hondo, E., Ogawa, K., Endo, H., Kimura, J., Yamada, J., Rerkamnuaychoke, W., Chungsamarnyart, N., Hayashi, Y., Nishida, T. (1996). An ultrastructural and lectin-histochemical study on the seminiferous epithelium of the common tree shrew (*Tupaia glis*). *J. Anat.*, 189(1): 87-95.

Abbreviations:

AAC:	Anterior acrosomal cap
AAS:	Anterior acrosomal segment
Ac:	Acrosomal Cap
Acr:	Acrosomal crown
AG:	Acrosomal granule
An:	Annulus
AS:	Anterior side of the nucleus
ANP:	Anterior nuclear protrusion
ANS:	Anterior nuclear shelf
ASS:	Anterior subacrosomal space
AV:	Acrosomal vesicle
AX:	Axoneme (Axial filament)
BM:	Basement membrane
BP:	Basal plate
CB:	Chromatoid body
CDD:	Crown dense diadems of the acrosome crown segments
CFE:	Caudal fusiform End of posterior acrosomal cap
Ch(s):	Chromatin(s)
ChD:	Chain of lateral dense diadems covering the acrosomal segments
CP:	Connecting piece
CS:	Crown segment of the acrosome
DAC:	Dorsal acrosomal cap
DC:	Distal centriole
DD:	Dense diadems of the acrosome crown segments
DNS:	Dorsal nuclear shelf
DS:	Dorsal side of the nucleus
EIP:	Early implantation fossa
ES:	Early spermatid
ETR:	electron translucent region
G:	Golgi body
GE:	Germinal epithelial cell
IF:	Implantation fossa
LDA:	Lateral dense arm
M:	Mitochondria
Mf:	microfilaments
MMs:	Manchette microtubules
MP:	Middle piece
MS:	Mitochondrial sheath
Mt:	Microtubule(s)
MtU:	Microtubule unit
N:	Nucleus
NC:	Nuclear constriction
NCa:	Nuclear canal(s)
NP:	Nuclear protrusion
NS:	Nuclear shelf
PAC:	Posterior limb of acrosomal cap
PAS:	Posterior acrosomal segment
PC:	Proximal centriole
PeS:	Pre-equatorial space
PFE:	Posterior fusiform end of the anterior acrosomal cap
PNP:	Posterior nuclear protrusion
PNS:	Posterior nuclear shelf
PP:	Posterior perinuclear space
PoS:	Posterior side of the nucleus
PS:	Enlarged posterior nuclear space
PSp:	Primary spermatocyte
PSS:	Posterior subacrosomal space
RER:	Rough endoplasmic reticulum
SAS:	Subacrosomal space
SC:	Subacrosomal cone
Ser:	Sertoli cell
SH:	Sperm head
SN:	Sperm neck
SV(s):	Secretory Vesicles
TC:	Terminal crest of acrosomal crown
TDR	Terminal dense rod
TS:	Terminal segment of acrosome
VAC:	Ventral acrosomal cap
VDP:	Ventrodorsal protrusion of the nucleus
VNS:	Ventral nuclear shelf
VS:	Visicular end of lateral acrosomal arm